Published in final edited form as:
Hematol Oncol Clin North Am. 2014 August ; 28(4): 747–764. doi:10.1016/j.hoc.2014.04.002.

Use of Magnetic Resonance Imaging to Monitor Iron Overload

John C. Wood, M.D. Ph.D.
Department of Pediatrics and Radiology, Children's Hospital, Los Angeles Keck School of Medicine, University of Southern Califorina

SYNOPSIS

Treatment of iron overload requires robust estimates of total body iron burden and its response to iron chelation therapy. Compliance with chelation therapy varies considerably among patients and individual reporting is notoriously unreliable. Even with perfect compliance, intersubject variability in chelator effectiveness is extremely high, necessitating reliable iron estimates to guide dose titration. In addition, each chelator has a unique profile with respect to clearing iron stores from different organs. This chapter will present the tools available to clinicians monitoring their patients, focusing on non-invasive magnetic resonance imaging methods because they have become the de-facto standard of care.

Keywords

Iron overload; thalassemia; sickle cell disease; chelation; MRI; iron; liver; heart

Monitoring transfusion burden

Each unit of packed red blood cells (PRBCs) contains 200 and 250 mg of iron. In fact, the iron can be calculated from the hematocrit (Hct) using the following relationship:

$$\text{Transfusional iron intake (ml/kg)} = \text{blood volume (ml/kg)} \times \text{Hct} \times 1.08 \quad (1)$$

where Hct is calculated from the PRBCs provided by the blood bank[1]. The volume of transfused blood in one year can be converted to a predicted change in liver iron concentration (LIC) if no chelation is taken using the following equation: [2]

$$\Delta\text{LIC} = \text{Transfusion iron intake}/10.6 \quad (2)$$

Thus a patient receiving 150 cc/kg/yr of PRBCs having a Hct of 70%, would increase their liver iron by 10 mg/g in the absence of iron chelation. As a rule of thumb, each 15 cc/kg transfusion will raise liver iron by ~1 mg/g dry weight.

Corresponding Author: John C. Wood, M.D. Ph.D., Cardiovascular MRI Lab, The Saban Research Institute, 4650 Sunset Boulevard, MS #34, Los Angeles, CA 90027, jwood@chla.usc.edu, Phone: 323-361-5470.

Therefore, tracking transfusional iron exposure is a logical and conceptually simple way of predicting iron chelation needs, a priori. It is clearly useful in deciding when to initiate iron chelation therapy. Systematic intensification of transfusion requirements, such as may occur during hepatitis C treatment, should prompt pre-emptive changes in iron chelation. However, there are two major limitations to using transfusional burden to adjust chelation. In practice, values may be difficult to track because amounts released from the blood bank are systematically larger than given to the patients. More importantly, there are complicated interactions between transfusion iron rate and chelator efficacy that may be patient and disease specific, creating differences between predicted and observed response to therapy.

Serum markers of iron overload

Ferritin is an intracellular iron storage protein that is essential for all living cells because it maintains labile cellular iron levels in a safe range, while protecting cells against iron deficiency in the future. The circulating serum ferritin pool mostly arises from the liver and reticuloendothelial systems and its biological role is unclear. The relationship between serum ferritin and total body iron stores is quite complicated. Correlation coefficients between ferritin and liver iron concentration are typically around 0.7, leaving 50% of the variability unexplained[3, 4]. More importantly, the confidence intervals for predicting LIC values from serum ferritin measurements are enormous. A patient having a serum ferritin of 1500 could have a LIC as low as 3 or as high as 30 mg/g dry weight. As a result, toxicity thresholds based upon serum ferritin levels can be dangerously misleading.

Why is serum ferritin so unreliable? Serum ferritin is an acute phase reactant[5] and rises sharply with inflammation. The liver is the major source of circulating ferritin and even minor liver insults will sharply increase serum ferritin[6]. In contrast, ascorbate deficiency leads to inappropriately low serum ferritin values relative to iron stores[7]. Lastly, serum ferritin levels depend on the transfusion rate as well as the body iron stores. Non-transfused iron overloaded patients, such as beta thalassemia intermedia patients, have much lower ferritin values for a given total body iron concentration[8].

Intrapatient trends in serum ferritin improve its predictive value[8]. We typically measure serum ferritin values with every transfusion and trend median values over a period of three to six months. Nonetheless, ferritin and LIC trends remain discordant more than 30% of the time[9]. Periods of discordance can span months to years[9].

Despite its limitations, serum ferritin is undoubtedly the most widely used method for tracking iron stores in the world because of its low cost and universal availability. Table 1 summarizes guidelines for improved use of serum ferritin to trend iron overload.

Transferrin saturation is also an important and widely available serologic marker of iron balance. It represents the earliest and most specific marker of primary hemochromatosis and is a key screening marker in all diagnostic algorithms for that disease[10]. Increased transferrin saturation can also be used as an indicator to initiate iron chelation therapy in thalassemia intermedia[11, 12] as well as all secondary hemochromatosis syndromes.

Many chronically transfused patients have fully saturated transferrin, making it uninformative for short and midterm assessment of chelation efficiency. The prevalence of circulating non-transferrin bound iron (NTBI) increases dramatically once transferrin saturation exceeds 85%[13]. Thus, desaturating transferrin below 85% is a reasonable long-term target for iron chelation therapy in transfusional siderosis syndromes. However from a practical perspective, transferrin saturation cannot be accurately assessed in the presence of circulating chelator so patients must hold their iron chelation for 24 hours prior to their blood draw, limiting the practicality of frequent monitoring by this method. We recommend annual screening of transferrin saturation in chronically transfused patients, at the same time as other screening laboratories.

Measurement of liver iron concentration (LIC)

The liver accounts for approximately 70%–80% of the total body iron stores in iron overloaded patients. As a result, changes in liver iron accurately predict the balance between transfusional burden and iron removal therapies[2, 14]. LIC exceeding 17 mg/g dry weight are associated with iron-mediated hepatocellular damage[15]. Patients with LIC values above this threshold are also at increased risk for cardiac iron overload[14, 16–18]. Long-term liver siderosis is associated in increased risk of hepatocellular carcinoma in patients with hereditary hemochromatosis[19]. Hepatocellular carcinoma is also becoming a leading cause of death in iron-loaded adults with thalassemia syndromes[20, 21], even in patients that are hepatitis C negative[8].

While increased LIC places patients at particular danger for iron overload complications, there is no “safe” LIC threshold below which cardiac and endocrine iron accumulation does not occur[22]. The reason for this apparent paradox is that many chronically transfused patients have fully-saturated transferrin, regardless of their LIC[13]. Patients who miss chelator doses expose their extrahepatic organs to unrestricted uptake of labile iron species[23].

Despite its limitations, LIC remains the best single metric for tracking chelator response and dosing adjustments. At most major thalassemia and sickle cell disease centers, it is measured annually to guide chelation therapy.

Liver Biopsy

Traditionally, LIC was measured by ultrasound guided transcutaneous needle biopsy. Biopsy has the advantage of providing both histologic assessment of liver damage and iron quantification. The complication rate is acceptable, typically about 0.5%, but life-threatening hemorrhages occur[24]. The single greatest limitation is the spatial heterogeneity of tissue iron deposition in the liver that can result in high sampling variability, even in the absence of significant liver disease. When significant fibrosis is present, the coefficient of variability can exceed 40%, making biopsy essentially useless for tracking response to therapy[25–27]. Following collection from a cutting needle, liver samples are fixed in formaldehyde and sent fresh or paraffin-embedded to special laboratories for quantification. Iron quantification is generally performed using tissue digestion in nitric acid followed by either atomic absorption or inductively coupled mass spectrometry. These assays have a

coefficient of variation of around 12%, independent of the sampling variability[28]. Values are reported as mg/g dry weight of tissue. Paraffin-embedded specimens must be dewaxed with organic solvents prior to digestion. This process lowers the tissue dry weight because it removes membrane lipids, raising the apparent iron concentration[29]. Because of its known systematic and random errors, cost, and invasiveness, liver biopsy can no longer be considered the “gold standard” for LIC assessment and should not be used except when tissue histology is necessary for diagnosis.

Computed Tomography

Iron increases X-ray attenuation proportionally to its concentration. The ability of carefully calibrated quantitative computed tomography (qCT) measurements to measure liver iron has been known for decades[30]. Two basic approaches used are single and dual energy techniques.

In single energy techniques, low dose qCT scan is performed in a middle hepatic level and the liver attenuation is compared to an external phantom control. The phantom need not be iron-based, it is simply necessary to correct for imperfections in the X-ray beam. The chief limitation of this approach is that changes in attenuation due to iron are small compared with normal attenuation fluctuations. Thus single energy qCT cannot accurately track LIC changes for LIC values less than 7 mg/g dry weight and is less accurate than MRI measurements for LIC values less than 15 or 20 mg/g[31, 32]. In contrast, qCT is quite robust for severe iron overload.

In dual energy techniques, measurements are performed at low and high Xray beam energies and the difference is used to predict the amount of iron. Non iron loaded tissue has similar attenuation values at both field strengths and is suppressed when the difference is calculated. While this potentially offers better discrimination at low iron concentrations, it requires higher radiation exposure to achieve this. Feasibility was demonstrated in animal studies nearly two decades ago[30, 32], but there have been no validation studies performed on modern equipment.

Magnetic Detectors

Tissue iron is paramagnetic. Consequently, devices that measure the magnetic properties of liver can quantify liver iron. The first devices to accomplish this used superconducting magnetic coils and were known as superconducting quantum interference devices (SQUIDs) [33, 34]. Although reasonably accurate, these devices are expensive, require specialized expertise for measurement acquisition and device maintenance, and can only quantitate iron in the liver and spleen. As a result, only four SQUID devices suitable for LIC quantification are operational, worldwide. More inexpensive devices that operate at room temperature could potentially become practical in the future, but remain research tools for the present[35].

MRI

Magnetic resonance imaging can also be used to quantify iron overload. It doesn’t measure liver iron directly, but its effect on water protons as they diffuse in the magnetically

inhomogeneous environment caused by iron deposition[36]. The principles are quite simple. The scanner transmits energy into the body in the form of microwaves, waits a period of time, and then actively recalls that energy as microwaves that are received by an antennae or "coil". The longer the scanner waits before recalling an echo, the less energy returns. This process is known as relaxation, and is characterized by the relaxation rates R2 and R2* (measured in Hz). These rates are just the mathematical inverse of the characteristic relaxation times, T2 and T2* (measured in ms). The higher the iron concentration, the higher the relaxation rates and the shorter the relaxation times. The difference between R2 and R2* depends upon how the scanner formed the echo. R2* is the parameter measured for gradient formed echoes but R2 is the parameter measured if radiofrequency pulses are used to form the echo (spin echo).

The first large study validating MRI as a means to quantify liver iron used a specific protocol to measure liver R2[37]. The R2 calibration curve was curvilinear and exhibited limits of agreement of −56% to 56%. Much of the uncertainty in this method arises from sampling errors of the "gold standard" liver biopsy, itself. Other sources of uncertainty are patient specific differences in iron distribution, speciation, and hepatic water content. However, liver R2 assessment is highly reproducible, has been independently validated[38], and is transferable across different types of MRI scanner. Figure 1 demonstrates work from our laboratory, independently confirming the initial R2-iron calibration. One specific liver R2 acquisition and analysis protocol, known as Ferriscan® has been FDA approved as a clinical device.

Figure 2 demonstrates the relationship between liver R2* and LIC. It is linear and has confidence intervals of −46% to 44%; calibration was independently validated in a subsequent study[39]. Some confusion exists in the literature because calculated R2* values depend until the type of mathematical models used to fit the MRI images. However, these biases are corrected when appropriate calibration curves are applied[40].

Both R2 and R2* are suitable for LIC estimates in clinical practice if performed using validated acquisition and analysis protocols. R2 and R2* are both more accurate than liver biopsy for determining response to iron chelation therapy[41]. However, it is important to use the same technique when tracking patients over time [42]. Liver R2* is more robust than liver R2 for tracking chelation response on time scales six months or shorter, but R2 and R2* performances are equivalent for annual examinations. Table 2 provides FDA approved options for R2 and R2* analysis. Some sites, including the author's, use software developed in-house. All such tools require cross-validation with established techniques prior to clinical use. Table 3 summarizes the advantages and disadvantages for both techniques.

Measurement of non-hepatic iron stores

While LIC is a terrific surrogate for total iron balance, it has limited ability to predict risk in extrahepatic organs. The endocrine glands and the heart develop pathologic iron overload exclusively through uptake of NTBI. The mechanism by which this uptake occurs is controversial, but L-type calcium channels have been implicated in some studies[43]. Regardless, it is possible for patients to develop progressive extrahepatic iron loading

despite iron chelation keeping them in neutral total iron balance[22, 44]. This is caused by the chelator having inadequate exposure to the chelatable iron pool, either because it doesn't enter the target organ or does not adequately suppress the circulating NTBI. Figure 3 demonstrates the LIC of 26 chronically transfused patients who developed de-novo cardiac iron load while under routine heart and liver iron surveillance at Children's Hospital Los Angeles, sorted by disease. All of the SCD patients had severe liver iron deposition before heart iron loading developed, while fewer than half of patients with other disease states had LIC's typically associated with cardiac iron. In fact, more than 40% of non-sickle patients had LIC's under 7 mg/g, a level thought to be "safe". Without routine cardiac surveillance, these patients would have ultimately developed endocrine and cardiac complications[45].

Heart Iron

The first paper linking MRI detectable cardiac iron to patient symptoms was in 2001. At that time, the calibration curves for cardiac iron were not known and results are displayed using the relaxation time, T2* (Figure 4a) [46]. T2* values greater than 20 ms are considered normal. All thalassemia major patients having T2* values in this range had normal ejection fraction. As T2* declined below 20 ms, there was an increasing prevalence of myocardial dysfunction, with a particularly high prevalence for T2* values less than 10 ms.

Cardiac T2* was initially validated against cardiac iron concentration in animal models[47] and later in two autopsy studies[48, 49]. Cardiac T2* values can be converted to cardiac iron concentration using the following equation:[49]

$$\text{Cardiac iron concentration} = 45/(\text{T2}^*)^{1.22} \quad (3)$$

Despite the availability of this equation, many papers continue to report results in T2* values because of physician familiarity with this metric.

The observation that many patients with cardiac iron loading had normal function puzzled initial investigators. However, MRI T2* is most sensitive to iron that is safely stored in hemosiderin deposits. Initially excess cardiac iron produces no ill effects because ferritin-hemosiderin buffering systems in the myocyte are able to keep the toxic labile cellular iron levels low. However, with time or ongoing loading, a tipping point is reached and cardiac symptoms developed. This was best demonstrated by a registry study[50] following 652 thalassemia patients from 21 centers in the United Kingdom (Figure 4b). The probability of developing congestive heart failure in one year's time was a powerful function of starting T2*, being less than 2% for a T2* value from 10–20 ms and greater than 50% for a T2* less than six milliseconds.

Based upon those findings, a "stoplight" scheme is often applied to cardiac T2* values: values greater than 20 ms are green, values between 10 and 20 ms are yellow, and values less than 10 ms are red. Many treatment paradigms use these designations including a recent consensus paper from the American Heart Association[51]. A commentary summarizing the development of MRI as the gold standard for cardiac iron quantification may also be found in a different issue of the same journal[52].

Pancreas Iron

Like the heart, the pancreas selectively takes up non-transferrin bound iron species[43], but it is a more sensitive predictor of long-term labile iron control[53]. Figure 5a depicts the relationship between pancreas R2* and heart R2*. Notice that there are regions where the pancreas is iron loaded with a clear heart, but the converse is never true. This reflects that pancreas is an early predictor of potential cardiac iron loading; a pancreas R2* of 100 Hz appears to represent a risk threshold[54]. Since the heart clears iron so slowly once it is loaded (half-life 14 months at maximal therapy, we recommend responding to unfavorable trends in pancreatic iron rather than waiting for cardiac iron to accumulate.

Pancreas R2* values also predict endocrine function[55]. Figure 5b demonstrates that the probability of having abnormal fasting glucose or oral glucose tolerance test (OGTT) increases as the pancreas and heart become iron loaded. While most of the patients with abnormal cardiac R2* also have overt diabetes, over 50% of the patients having isolated pancreas iron overload manifested preclinical glucose dysregulation by OGTT.

Pituitary Iron

Hypogonadal hypogonadism remains the leading endocrinopathy in thalassemia major patients, with a prevalence of approximately 50% in multicenter trials[56, 57]. Although improved access to iron chelation is undoubtedly lowering that figure, monitoring of pituitary function cannot begin until puberty. Unfortunately, significant iron accumulation occurs during the first and second decades of life, producing irreversible gland destruction in early adulthood[58]. Pituitary iron accumulation is correlated with iron deposition in the liver, pancreas, and heart. Heart deposition is late, however, and patients with increased cardiac iron are at high risk for hypogonadism[58].

Since hypogonadism is only partially reversible with intensive chelation[59], it is imperative to identify and treat preclinical pituitary iron deposition. Since the pituitary resides in a magnetically inhomogenous environment (in the sella tursica), R2 imaging, rather than R2* imaging is indicated. Imaging protocols for pituitary R2 and pituitary volume assessment are well established[60], and age and sex specific normative values have been published. A Z_{vol} value < −2 indicates gland shrinkage below the 2.5^{th} percentile and a Z_{R2} value > 2 indicates iron accumulation > 97.5^{th} percentile.

Risk thresholds for pituitary iron accumulation and gland shrinkage are demonstrated in Figure 6. Z_{R2} values less than −2.5 were associated with a high rate (88%) of hypogonadism. Moderate pituitary iron deposition ($2 < Z_{R2} < 5$) was not associated with clinical hypogonadism in this study, but biochemical hypogonadism was not assessed. In contrast, 50% of the patients have severe pituitary iron deposition ($Z_{R2} > 5$) were hypogonadal.

Standards for routine monitoring have not been established. We recommend one scan between 7 and 10 years of age to identify patients with early onset pituitary iron deposition. The second and early third decade are particularly dynamic from both a physiologic and emotional perspective. Monitoring is particularly important to identify and correct problems that may block the critical period for sexual and bone development.

We have also used these techniques to probe intermittently transfused children with hypogonadism following bone marrow transplantation, head irradiation, or chemotherapy for acute myelogenous leukemia. Although results remain anecdotal, gland shrinkage also appears to have a high specificity for hypogonadism of for non-iron mediated pituitary toxicities.

Kidney iron

The most common source of iron deposition in the kidney is intravascular hemolysis. Decellularized hemoglobin (also known as plasma free hemoglobin) is filtered at the glomerulus and actively taken up by megalin-cubulin receptors in the proximal and distal convoluted tubules[61]. This creates a characteristic cortical darkening on MRI images, with complete sparing of the medulla[62]. Global kidney R2* values can reach 200 Hz, with cortical values more than 1000 Hz, and are correlated with surrogates of hemolysis such as LDH[63]. No correlations have been observed between kidney R2* and liver iron concentration in patients with hemolytic disease. Functional significance of renal iron deposits remain unproven, although no longitudinal studies have been performed to date.

Mild kidney R2* increases can also be observed in non-hemolytic anemias, but the iron deposition is not limited to the cortex. R2* values rarely exceed 60 Hz and these mild elevations are typically only observed for severe LIC elevations. These changes may represent NTBI uptake and storage throughout the different renal cell-types, as has been described on autopsy studies, but functional significance remains controversial.

Spleen iron

Spleen R2* values are easy to measure using the same analysis and acquisition techniques as the liver. No R2* – iron calibration curve has been directly validated, but indirect methods have been applied[64]. No functional significance for spleen iron accumulation has been determined to date.

Impact of disease state on extrahepatic iron loading

Primary hemochromatosis and thalassemia intermedia syndromes are typically characterized by sparing of reticuloendothelial organs, like the spleen, and only rarely lead to cardiac and endocrine involvement. Extrahepatic deposition doesn’t typically occur until the fourth or fifth decade of life, usually after significant hepatic damage has already occurred.

In contrast, transfusional siderosis loads the bone-marrow and reticuloendothelial system first, with liver parenchymal, endocrine, and cardiac iron loading later in that order. However, the risk of extrahepatic iron loading varies considerably across different anemia subtypes. One of the strongest predictors is the rate of effective red cell production, reflected by the reticulocyte count. Red cell production requires transferrin-bound uptake into the bone marrow erythroid precursors, regenerating apo-transferrin and lowering transferrin saturation. Blackfan-Diamond patients, which have the lowest transferrin utilizations of any anemia, are particularly prone to cardiac and endocrine iron deposition. They may develop cardiac iron within just a first few years after starting transfusion therapy[65, 66]. Congenital dyserythropoetic anemia, thalassemia major and aplastic anemia patients have

intermediate risk, with cardiac iron typically occurring no less than seven to ten years after initiating transfusions when receiving appropriate transfusion and chelation therapy[66]. Sickle cell disease patients represent the lowest risk category[67]. Many SCD patients retain high reticulocyte counts during chronic transfusion therapy, leading to lower transferrin saturations, and circulating labile plasma iron levels[64]. Cardiac and endocrine iron deposition do occur in SCD, but later in life and at a slower rate than chronically transfused thalassemia patients[68].

Rational monitoring practices

MRI is a relatively expensive procedure and care must be made to use the resource wisely. However, monitoring costs are relatively modest compared to cost of iron chelation medications and the cost of iron-mediated complications. Figure 7 is a flow chart outlining our clinical practice. Sometimes we have sufficient clinical knowledge to assign risk purely based on the patients disease state, transfusion intensity, access to chelation, or MRI results from another institution. For example, our “low risk” patients include most sickle cell disease patients and transfusion independent patients with iron overload. Low risk patients only need MRI examination of the abdomen, because a “clean” pancreas guarantees that the heart is free from significant iron deposition. We define a “intermediate” risk patient as chronically transfused and having sufficient transfusional exposure (usually greater 7 years for a thalassemia major patient) to be at risk for cardiac iron overload. However, most patients receive heart and abdominal MRI examinations on the first visit because we are unsure of their complete transfusion and chelation history and because there can be genetic co-modifiers of cardiac risk.

High risk patients are defined as those whose cardiac T2* is less than 10 ms. We scan these patients at six month intervals for three reasons. Firstly, it is important to monitor their left ventricular function. We treat even minor decreases in ventricular function quite aggressively. Secondly, liver iron can change quite quickly during intensified therapy and it is important to avoid overchelation. Lastly, it provides important feedback to the patients who often struggle drug compliance.

Availability of MRI iron assessments

With increased recognition of the utility of MRI in iron overload syndromes, the availability of individual medical centers to assess liver and cardiac iron is growly daily. Many radiology departments prefer to do the analyses themselves because there are financial and intellectual incentives to do so. However, quality control remains a significant problem in this regard unless the imaging centers take proper care to validate their acquisition techniques and their readers.

Some imaging centers are not interested in devoting the time necessary to maintain clinical competence in these metrics because imaging volume does not justify the financial overhead. In these situations, third party solutions represent a “win-win” situation for radiology departments and practitioners interested in liver iron and cardiac T2* measurements.

Measurement of pancreatic R2* can be performed using the same techniques as for liver R2*. Fatty replacement of the gland complicates measurements in older subjects and measurement variability is higher than the other organs. Also, pancreas orientation is highly variable in splenectomized subjects, making measurement more challenging. Thus pancreas R2* measurements are not universally obtained, but are gaining increasing acceptance. Our laboratory is exploring novel methods to improve access to these techniques.

Pituitary R2 is also not universally performed. It is a relatively easy and fast measurement to obtain (4 minutes). Post-processing is also more straightforward than for the liver, making it easy for most radiology departments to perform adequately. However, the iron overload field is evolving so rapidly that a clinical niche for pituitary R2 assessments has not been firmly established. However, as more experimental data and clinical experience accumulate, pituitary R2 measurements are likely to increase in importance, especially in sickle cell disease and survivors of pediatric malignancy.

Summary

Serum ferritin and transferrin saturation remain valuable in tracking the therapeutic response to iron removal therapies. However, these inexpensive techniques have many shortcomings that preclude using them safely as sole monitors for chelator efficacy. MRI has become the de-facto gold standard for tracking iron levels in the body because it is accurate, reproducible, well tolerated by patients and can track iron levels in different organs of the body. The latter characteristic is important because the mechanisms and kinetics of iron uptake and clearance varies across somatic organs. We present our clinical practice as a reference but individual experiences will still be colored by local expertise as the technologies continue to mature and distribute.

References

1. Cohen AR, Glimm E, Porter JB. Effect of transfusional iron intake on response to chelation therapy in beta-thalassemia major. Blood. 2008; 111:583–587. [PubMed: 17951527]
2. Angelucci E, Brittenham GM, McLaren CE, et al. Hepatic iron concentration and total body iron stores in thalassemia major. New England Journal of Medicine. 2000; 343:327–331. [PubMed: 10922422]
3. Brittenham GM, Cohen AR, McLaren CE, et al. Hepatic iron stores and plasma ferritin concentration in patients with sickle cell anemia and thalassemia major. Am J Hematol. 1993; 42:81–85. [PubMed: 8416302]
4. Belhoul KM, Bakir ML, Saned MS, et al. Serum ferritin levels and endocrinopathy in medically treated patients with beta thalassemia major. Ann Hematol. 2012; 91:1107–1114. [PubMed: 22281991]
5. Herbert V, Jayatilleke E, Shaw S, et al. Serum ferritin iron, a new test, measures human body iron stores unconfounded by inflammation. Stem Cells. 1997; 15:291–296. [PubMed: 9253113]
6. Kountouras D, Tsagarakis NJ, Fatourou E, et al. Liver disease in adult transfusion-dependent beta-thalassaemic patients: investigating the role of iron overload and chronic HCV infection. Liver Int. 2013; 33:420–427. [PubMed: 23402611]
7. Chapman RW, Hussain MA, Gorman A, et al. Effect of ascorbic acid deficiency on serum ferritin concentration in patients with beta-thalassaemia major and iron overload. J Clin Pathol. 1982; 35:487–491. [PubMed: 7085892]
8. Musallam KM, Cappellini MD, Wood JC, et al. Iron overload in non-transfusion-dependent thalassemia: a clinical perspective. Blood Rev. 2012; 26(Suppl 1):S16–19. [PubMed: 22631036]

9. Puliyel M, Sposto R, Berdoukas VA, et al. Ferritin trends do not predict changes in total body iron in patients with transfusional iron overload. Am J Hematol. 2013
10. Crownover BK, Covey CJ. Hereditary hemochromatosis. Am Fam Physician. 2013; 87:183–190. [PubMed: 23418762]
11. Wangruangsathit S, Hathirat P, Chuansumrit A, et al. The correlation of transferrin saturation and ferritin in non-splenectomized thalassemic children. J Med Assoc Thai. 1999; 82(Suppl 1):S74–76. [PubMed: 10730522]
12. Pootrakul P, Breuer W, Sametband M, et al. Labile plasma iron (LPI) as an indicator of chelatable plasma redox activity in iron-overloaded beta-thalassemia/HbE patients treated with an oral chelator. Blood. 2004; 104:1504–1510. [PubMed: 15155464]
13. Piga A, Longo F, Duca L, et al. High nontransferrin bound iron levels and heart disease in thalassemia major. Am J Hematol. 2009; 84:29–33. [PubMed: 19006228]
14. Brittenham GM, Griffith PM, Nienhuis AW, et al. Efficacy of deferoxamine in preventing complications of iron overload in patients with thalassemia major. New England Journal of Medicine. 1994; 331:567–573. [PubMed: 8047080]
15. Angelucci E, Muretto P, Nicolucci A, et al. Effects of iron overload and hepatitis C virus positivity in determining progression of liver fibrosis in thalassemia following bone marrow transplantation. Blood. 2002; 100:17–21. [PubMed: 12070002]
16. Jensen PD, Jensen FT, Christensen T, et al. Evaluation of myocardial iron by magnetic resonance imaging during iron chelation therapy with deferrioxamine: indication of close relation between myocardial iron content and chelatable iron pool. Blood. 2003; 101:4632–4639. [PubMed: 12576333]
17. Wood JC, Kang BP, Thompson A, et al. The effect of deferasirox on cardiac iron in thalassemia major: impact of total body iron stores. Blood. 2010; 116:537–543. [PubMed: 20421452]
18. Telfer PT, Prestcott E, Holden S, et al. Hepatic iron concentration combined with long-term monitoring of serum ferritin to predict complications of iron overload in thalassaemia major. British Journal of Haematology. 2000; 110:971–977. [PubMed: 11054091]
19. Kanwar P, Kowdley KV. Diagnosis and treatment of hereditary hemochromatosis: an update. Expert Rev Gastroenterol Hepatol. 2013; 7:517–530. [PubMed: 23985001]
20. Mancuso A. Hepatocellular carcinoma in thalassemia: A critical review. World J Hepatol. 2010; 2:171–174. [PubMed: 21160991]
21. Mancuso A. Management of hepatocellular carcinoma: Enlightening the gray zones. World J Hepatol. 2013; 5:302–310. [PubMed: 23805354]
22. Noetzli LJ, Carson SM, Nord AS, et al. Longitudinal analysis of heart and liver iron in thalassemia major. Blood. 2008; 112:2973–2978. [PubMed: 18650452]
23. Wood JC, Glynos T, Thompson A, et al. Relationship between LPI, LIC, and cardiac response in a deferasirox monotherapy trial. Haematologica. 2011
24. Angelucci E, Baronciani D, Lucarelli G, et al. Needle liver biopsy in thalassaemia: analyses of diagnostic accuracy and safety in 1184 consecutive biopsies. Br J Haematol. 1995; 89:757–761. [PubMed: 7772512]
25. Ambu R, Crisponi G, Sciot R, et al. Uneven hepatic iron and phosphorus distribution in beta-thalassemia. Journal of Hepatology. 1995; 23:544–549. [PubMed: 8583142]
26. Emond MJ, Bronner MP, Carlson TH, et al. Quantitative study of the variability of hepatic iron concentrations. Clinical Chemistry. 1999; 45:340–346. [PubMed: 10053034]
27. Villeneuve JP, Bilodeau M, Lepage R, et al. Variability in hepatic iron concentration measurement from needle-biopsy specimens. J Hepatol. 1996; 25:172–177. [PubMed: 8878778]
28. Koh TS, Benson TH, Judson GJ. Trace element analysis of bovine liver: interlaboratory survey in Australia and New Zealand. J Assoc Off Anal Chem. 1980; 63:809–813. [PubMed: 7400087]
29. Butensky E, Fischer R, Hudes M, et al. Variability in hepatic iron concentration in percutaneous needle biopsy specimens from patients with transfusional hemosiderosis. Am J Clin Pathol. 2005; 123:146–152. [PubMed: 15762291]
30. Goldberg HI, Cann CE, Moss AA, et al. Noninvasive quantitation of liver iron in dogs with hemochromatosis using dual-energy CT scanning. Investigative Radiology. 1982; 17:375–380. [PubMed: 7129818]

31. Wood JC, Mo A, Gera A, et al. Quantitative computed tomography assessment of transfusional iron overload. Br J Haematol. 2011; 153:780–785. [PubMed: 21517807]
32. Nielsen P, Engelhardt R, Fischer R, et al. Noninvasive liver-iron quantification by computed tomography in iron-overloaded rats. Invest Radiol. 1992; 27:312–317. [PubMed: 1601623]
33. Brittenham GM, Farrell DE, Harris JW, et al. Magnetic-susceptibility measurement of human iron stores. N Engl J Med. 1982; 307:1671–1675. [PubMed: 7144866]
34. Fischer R, Longo F, Nielsen P, et al. Monitoring long-term efficacy of iron chelation therapy by deferiprone and desferrioxamine in patients with beta-thalassaemia major: application of SQUID biomagnetic liver susceptometry. Br J Haematol. 2003; 121:938–948. [PubMed: 12786807]
35. Gianesin B, Zefiro D, Musso M, et al. Measurement of liver iron overload: noninvasive calibration of MRI-R2* by magnetic iron detector susceptometer. Magn Reson Med. 2012; 67:1782–1786. [PubMed: 22135193]
36. Ghugre NR, Wood JC. Relaxivity-iron calibration in hepatic iron overload: probing underlying biophysical mechanisms using a Monte Carlo model. Magn Reson Med. 2011; 65:837–847. [PubMed: 21337413]
37. St Pierre TG, Clark PR, Chua-anusorn W, et al. Noninvasive measurement and imaging of liver iron concentrations using proton magnetic resonance. Blood. 2005; 105:855–861. [PubMed: 15256427]
38. Wood JC, Enriquez C, Ghugre N, et al. MRI R2 and R2* mapping accurately estimates hepatic iron concentration in transfusion-dependent thalassemia and sickle cell disease patients. Blood. 2005; 106:1460–1465. [PubMed: 15860670]
39. Hankins JS, McCarville MB, Loeffler RB, et al. R2* magnetic resonance imaging of the liver in patients with iron overload. Blood. 2009; 113:4853–4855. [PubMed: 19264677]
40. Meloni A, Rienhoff HY Jr, Jones A, et al. The use of appropriate calibration curves corrects for systematic differences in liver R2* values measured using different software packages. Br J Haematol. 2013; 161:888–891. [PubMed: 23496418]
41. Wood JC, Zhang P, Rienhoff H, et al. Liver MRI is better than biopsy for assessing total boday iron balance: validation by simulation. Blood. 2013; 122:958. [PubMed: 23814019]
42. Wood JC, Zhang P, Rienhoff H, et al. R2 and R2* are equally effective in evaluating Chronic response to iron chelation. Am J Hematol. 2014
43. Oudit GY, Trivieri MG, Khaper N, et al. Role of L-type Ca2+ channels in iron transport and iron-overload cardiomyopathy. J Mol Med. 2006; 84:349–364. [PubMed: 16604332]
44. Anderson LJ, Westwood MA, Prescott E, et al. Development of thalassaemic iron overload cardiomyopathy despite low liver iron levels and meticulous compliance to desferrioxamine. Acta Haematol. 2006; 115:106–108. [PubMed: 16424659]
45. Gabutti V, Piga A. Results of long-term iron-chelating therapy. Acta Haematol. 1996; 95:26–36. [PubMed: 8604584]
46. Anderson LJ, Holden S, Davis B, et al. Cardiovascular T2-star (T2*) magnetic resonance for the early diagnosis of myocardial iron overload. Eur Heart J. 2001; 22:2171–2179. [PubMed: 11913479]
47. Wood JC, Otto-Duessel M, Aguilar M, et al. Cardiac iron determines cardiac T2*, T2, and T1 in the gerbil model of iron cardiomyopathy. Circulation. 2005; 112:535–543. [PubMed: 16027257]
48. Ghugre NR, Enriquez CM, Gonzalez I, et al. MRI detects myocardial iron in the human heart. Magnetic Resonance in Medicine. 2006; 56:681–686. [PubMed: 16888797]
49. Carpenter JP, He T, Kirk P, et al. On T2* Magnetic Resonance and Cardiac Iron. Circulation. 2011
50. Kirk P, Roughton M, Porter JB, et al. Cardiac T2* magnetic resonance for prediction of cardiac complications in thalassemia major. Circulation. 2009; 120:1961–1968. [PubMed: 19801505]
51. Pennell DJ, Udelson JE, Arai AE, et al. Cardiovascular Function and Treatment in beta-Thalassemia Major: A Consensus Statement From the American Heart Association. Circulation. 2013
52. Wood JC. History and current impact of cardiac magnetic resonance imaging on the management of iron overload. Circulation. 2009; 120:1937–1939. [PubMed: 19884464]

53. Noetzli LJ, Coates TD, Wood JC. Pancreatic iron loading in chronically transfused sickle cell disease is lower than in thalassaemia major. Br J Haematol. 2011; 152:229–233. [PubMed: 21118197]
54. Noetzli LJ, Papudesi J, Coates TD, et al. Pancreatic iron loading predicts cardiac iron loading in thalassemia major. Blood. 2009; 114:4021–4026. [PubMed: 19726718]
55. Noetzli LJ, Mittelman SD, Watanabe RM, et al. Pancreatic iron and glucose dysregulation in thalassemia major. Am J Hematol. 2012; 87:155–160. [PubMed: 22120775]
56. Borgna-Pignatti C, Rugolotto S, De Stefano P, et al. Survival and complications in patients with thalassemia major treated with transfusion and deferoxamine. Haematologica. 2004; 89:1187–1193. [PubMed: 15477202]
57. Vogiatzi MG, Macklin EA, Trachtenberg FL, et al. Differences in the prevalence of growth, endocrine and vitamin D abnormalities among the various thalassaemia syndromes in North America. Br J Haematol. 2009; 146:546–556. [PubMed: 19604241]
58. Noetzli LJ, Panigrahy A, Mittelman SD, et al. Pituitary iron and volume predict hypogonadism in transfusional iron overload. Am J Hematol. 2012; 87:167–171. [PubMed: 22213195]
59. Farmaki K, Tzoumari I, Pappa C, et al. Normalisation of total body iron load with very intensive combined chelation reverses cardiac and endocrine complications of thalassaemia major. Br J Haematol. 2010; 148:466–475. [PubMed: 19912219]
60. Noetzli LJ, Panigrahy A, Hyderi A, et al. Pituitary iron and volume imaging in healthy controls. AJNR Am J Neuroradiol. 2012; 33:259–265. [PubMed: 22081683]
61. Gburek J, Birn H, Verroust PJ, et al. Renal uptake of myoglobin is mediated by the endocytic receptors megalin and cubilin. Am J Physiol Renal Physiol. 2003; 285:F451–458. [PubMed: 12724130]
62. Solecki R, von Zglinicki T, Muller HM, et al. Iron overload of spleen, liver and kidney as a consequence of hemolytic anaemia. Exp Pathol. 1983; 23:227–235. [PubMed: 6683665]
63. Schein A, Enriquez C, Coates TD, et al. Magnetic resonance detection of kidney iron deposition in sickle cell disease: A marker of chronic hemolysis. J Magn Reson Imaging. 2008; 28:698–704. [PubMed: 18777554]
64. Brewer CJ, Coates TD, Wood JC. Spleen R2 and R2* in iron-overloaded patients with sickle cell disease and thalassemia major. J Magn Reson Imaging. 2009; 29:357–364. [PubMed: 19161188]
65. Porter JB. Concepts and goals in the management of transfusional iron overload. Am J Hematol. 2007; 82:1136–1139. [PubMed: 17968973]
66. Wood JC, Origa R, Agus A, et al. Onset of cardiac iron loading in pediatric patients with thalassemia major. Haematologica. 2008; 93:917–920. [PubMed: 18413890]
67. Wood JC, Tyszka JM, Ghugre N, et al. Myocardial iron loading in transfusion-dependent thalassemia and sickle-cell disease. Blood. 2004; 103:1934–1936. [PubMed: 14630822]
68. Meloni A, Puliyel M, Pepe A, et al. Cardiac iron overload in sickle cell anemia. Blood. 2013; 122:1013.
69. Wood JC. Magnetic resonance imaging measurement of iron overload. Curr Opin Hematol. 2007; 14:183–190. [PubMed: 17414205]
70. Garbowski M, Carpenter JP, Smith G, et al. Calibration of Improved T2* Method for the Estimation of LIver Iron Concentration in Transfusional Iron Overload. Blood. 2009; 114

- Serum ferritin and transferrin saturation remain valuable in tracking the therapeutic response to iron removal therapies.
- These inexpensive techniques have many shortcomings that preclude using them safely as sole monitors for chelator efficacy.
- MRI has become the de-facto gold standard for tracking iron levels in the body because it is accurate, reproducible, well tolerated by patients and can track iron levels in different organs of the body.
- The latter characteristic is important because the mechanisms and kinetics of iron uptake and clearance varies across somatic organs.
- We present our clinical practice as a reference but individual experiences will still be colored by local expertise as the technologies continue to mature and distribute.

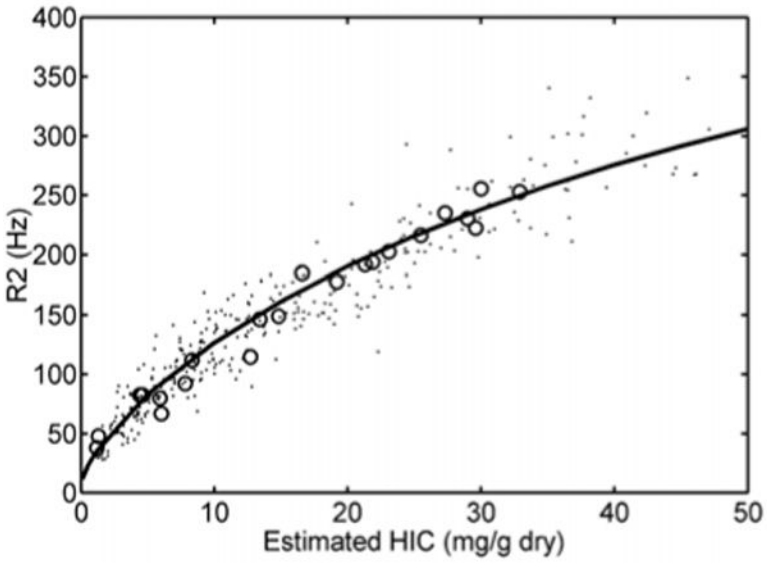

Figure 1.

Scattergram of liver R2 as a function of LIC by biopsy (open circles), or by liver R2* (dots) [38, 69]. Solid line represents the calibration curve originally published by St Pierre[37], et al, not a fit to the data. Despite significant differences in scanner hardware, image acquisition, and post-processing techniques between the two laboratories, the overall agreement is excellent.

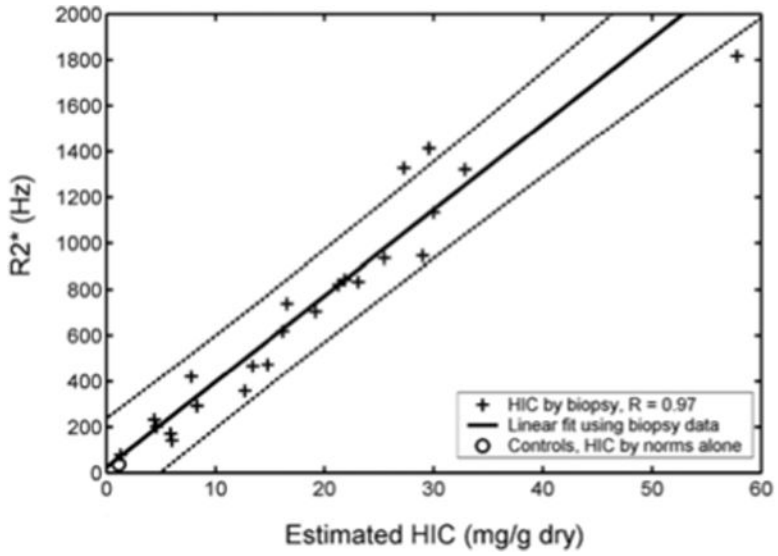

Figure 2.

(Left) Scattergram of liver R2* as a function of LIC by biopsy. Relationship is linear, with confidence intervals of −46% to 44% [38]. Calibration curve was independently validated[39].

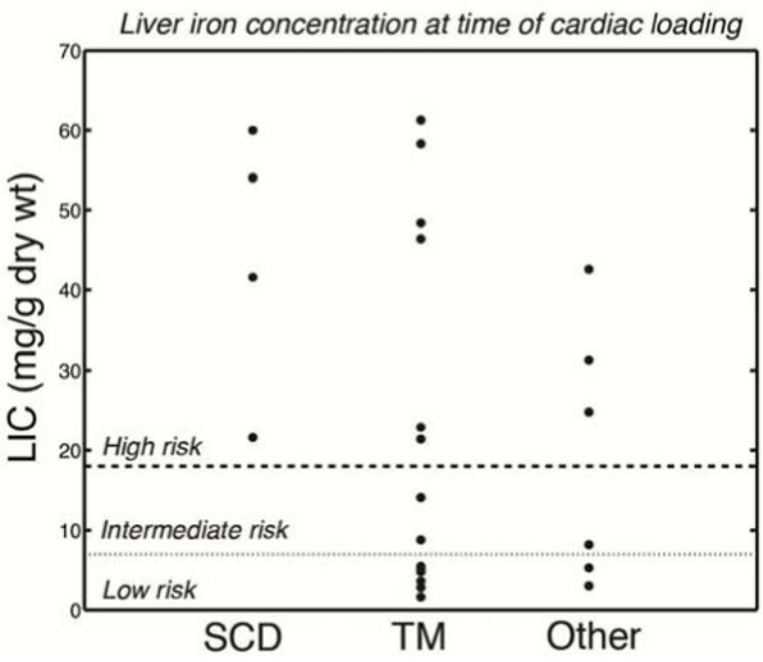

Figure 3.

Graph demonstrating LIC value (in mg/g dry weight) measured at the time heart iron became detectable. LIC values greater than 18 mg/g were considered high risk and LIC values between 7 mg/g and 18 mg/g assigned intermediate risk.

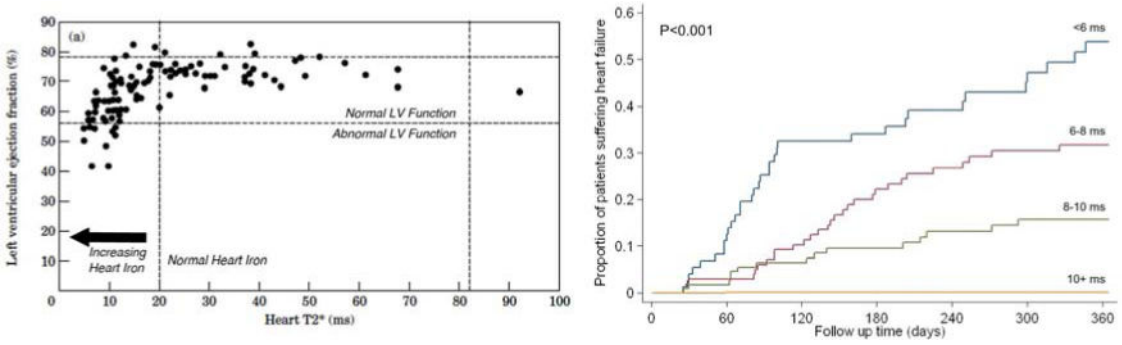

Figure 4.

(Left) Plot of left ventricular ejection fraction (in percent) versus heart T2* (in milliseconds). A T2* greater than 20 ms indicates that the heart is free of cardiac iron. Ejection fraction above 56% is considered normal. As heart iron increases (T2* declines) the prevalence of abnormal function increases [46]. (Right) Probability of developing clinical heart failure over a one year interval, based upon initial cardiac T2*. Cardiac T2* < 6 ms was associated with nearly a 50% likelihood of developing heart failure over one year [50].

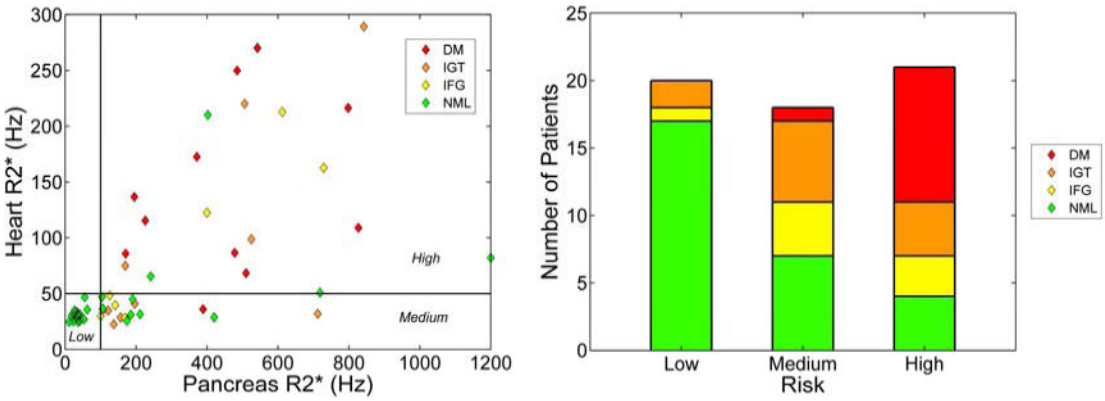

Figure 5.

(Left) Plot of heart R2* versus pancreas R2*[55]. Horizontal line at 50 Hz indicates the threshold of detectable heart iron. Vertical line at 100 Hz represents a risk threshold for pancreas R2*. Color of each diamond represents the outcome of an oral glucose tolerance test. Normal heart and normal pancreas represents low risk. Normal heart with abnormal pancreas represents medium risk. When both organs have iron overload, the patient is considered high risk. (Right) Results of OGTT test as a function of risk threshold[55].

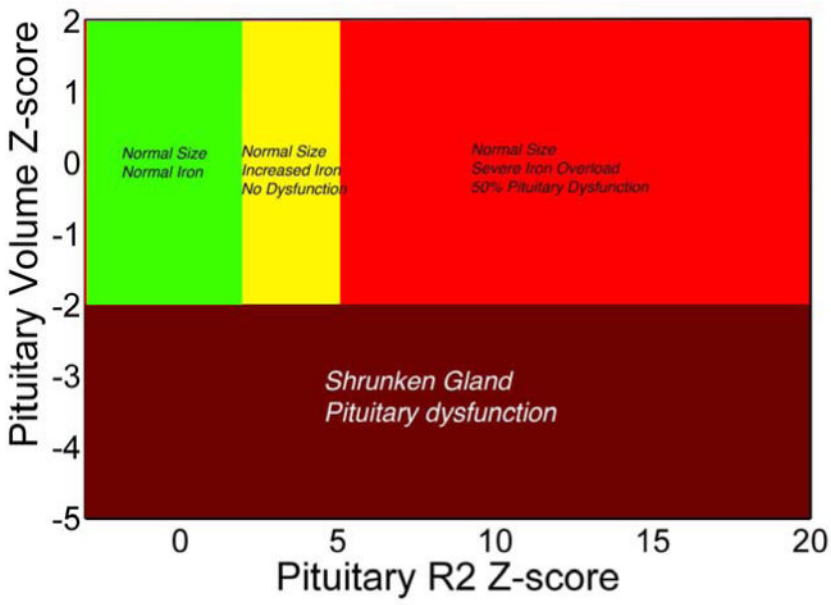

Figure 6.

Plot of pituitary size (Z-score) versus pituitary iron[58, 60]. No pituitary dysfunction was observed when size and iron Z-scores were normal (green) or even when pituitary iron was moderately elevated (Z score 2 to 5, yellow zone)[58]. However, hypogonadism was common (50%) in severe pituitary iron overload (Z > 5, red zone) or when the pituitary gland was shrunken (Z score < −2.0).

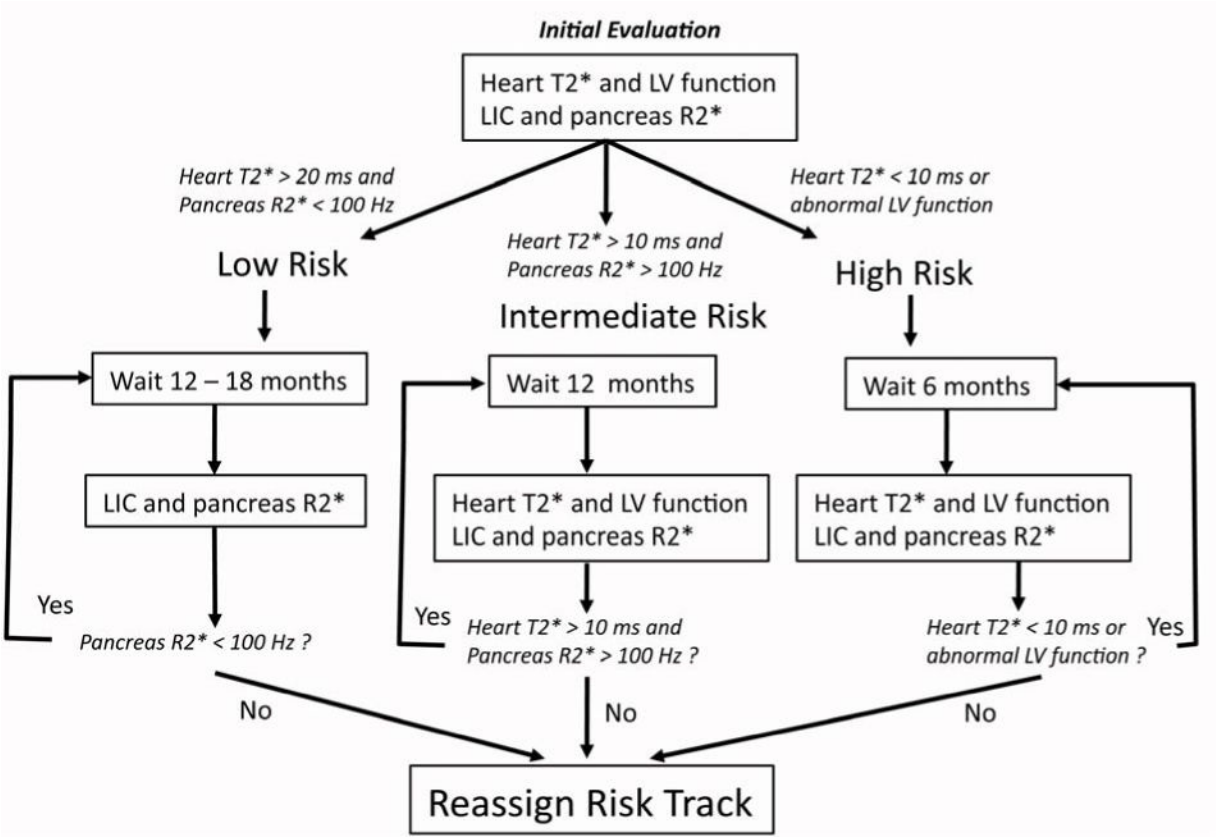

Figure 7.

Flow chart outlining our recommended monitoring algorithm. If there is insufficient clinical data to assign patients to a given monitoring track, all patients will undergo a baseline liver and heart iron examination for staging of clinical risk based upon their cardiac T2* and pancreas R2* values. After each subsequent MRI examination, patients are re-stratified, as necessary, to the appropriate monitoring track.

Table 1

Guidelines for use of serum ferritin to monitor iron balance

1	Measure serum ferritin every or every other transfusion visit for transfused patients and quarterly for nontransfused patients.
2	Calculate median values over 3–6 month intervals for trends
3	Monitor and prevent ascorbate deficiency
4	Anchor each serum ferritin trends to LIC assessments at a minimum of every two years.
5	Repeat MRI if trends in serum ferritin are incongruent with reported patient compliance or other clinical assessments

Table 2

FDA approved imaging companies and analysis software

Tool	Description
Ferriscan	A full service imaging company that will guide tightly controlled image acquisition and provide an imaging report. A good option when local radiology expertise or interest is lacking. Billed as a charge per exam that must be passed to insurers or patients.
CMR Tools Circle CMR42 Diagnosoft STAR Medis QMass	Standalone software that provides organ T2* measurements from suitably acquired images. Care must be taken to measure regions and truncate signal decay curves appropriately. Values are not reported in iron units but calibration curves for liver and heart may be found in [70]and [49]. Software can be licensed annually or purchased outright.
ReportCard	MRI vendor-based T2* analysis packages. Some allow use of different fitting models. Cross-validation with other techniques is lacking for these tools at the present. Software is generally purchased outright at the time of equipment acquisition.

Table 3

Advantages and disadvantages of Ferriscan R2 versus R2* analysis

	Ferriscan R2	**R2***
Speed	10 minutes per exam	< 1 minute
Validation	++++	++++
Reproducibility	5–8%	5–6%
Quality Control	Tight (by vendor)	Variable (by site)
Cost	$400 per exam	Variable. Approximately 10 minutes of technician time + software costs
Dynamic range	0–43 mg/g	Variable, usually 0 to 35 mg/g
Breathing artifact	Vulnerable to ghosting	Robust (breath-hold)
Metal/gas artifact	Robust	May affect usable region.